Cerebral Cortex, April 2020;30: 2114–2127

doi: 10.1093/cercor/bhz226
Advance Access Publication Date: 6 December 2019
Original Article

ORIGINAL ARTICLE

Ultrastructural Evidence for a Role of Astrocytes and Glycogen-Derived Lactate in Learning-Dependent Synaptic Stabilization

E. Vezzoli[1,2,3,†], C. Calì[1,†], M. De Roo[4,†], L. Ponzoni[3,†], E. Sogne[1], N. Gagnon[1], M. Francolini[3], D. Braida[3], M. Sala[5], D. Muller[4,#], A. Falqui[1,*] and P. J. Magistretti[1,*]

[1]Biological and Environmental Sciences and Engineering (BESE) Division, King Abdullah University of Science and Technology (KAUST), 23955-6900 Thuwal, Saudi Arabia, [2]Dipartimento di Bioscienze, Università degli Studi di Milano, 20133 Milano, Italy, [3]Dipartimento di Biotecnologie Mediche e Medicina Traslazionale, Università degli Studi di Milano, 20133 Milano, Italy, [4]Department of Basic Neuroscience, University of Geneva Medical School, 1206 Geneva, Switzerland, and [5]CNR, Institute of Neuroscience, 20129 Milano, Italy

Address correspondence to Andrea Falqui. Email andrea.falqui@kaust.edu.sa; Pierre J. Magistretti. Email pierre.magistretti@kaust.edu.sa
[†]These Authors Contributed Equally.
[#]Deceased.

Downloaded from https://academic.oup.com/cercor/article-abstract/30/4/2114/5625994 by guest on 24 June 2020

Abstract

Long-term memory formation (LTM) is a process accompanied by energy-demanding structural changes at synapses and increased spine density. Concomitant increases in both spine volume and postsynaptic density (PSD) surface area have been suggested but never quantified in vivo by clear-cut experimental evidence. Using novel object recognition in mice as a learning task followed by 3D electron microscopy analysis, we demonstrate that LTM induced all aforementioned synaptic changes, together with an increase in the size of astrocytic glycogen granules, which are a source of lactate for neurons. The selective inhibition of glycogen metabolism in astrocytes impaired learning, affecting all the related synaptic changes. Intrahippocampal administration of L-lactate rescued the behavioral phenotype, along with spine density within 24 hours. Spine dynamics in hippocampal organotypic slices undergoing theta burst-induced long-term potentiation was similarly affected by inhibition of glycogen metabolism and rescued by L-lactate. These results suggest that learning primes astrocytic energy stores and signaling to sustain synaptic plasticity via L-lactate.

Key words: 3D electron microscopy, glycogen metabolism, lactate, long-term memory, synaptic plasticity

Introduction

The brain represents only 2% of the body mass while consuming 20 to 25% of the total body energy (Raichle and Gusnard 2002; Magistretti and Allaman 2013). Recent estimates report that an adult human brain contains an impressive hundred trillion synapses in total (Drachman 2005). Synaptic activity accounts for approximately 70% of brain energy budget (Harris et al. 2012).

The signals detected by functional brain imaging techniques, such as positron emission tomography and functional magnetic resonance imaging, are based on metabolic (glucose and oxygen consumption) and vascular (blood flow and oxygenation level) processes associated with neuronal activity, offering a surrogate readout of neuronal and synaptic activity (Shulman and Rothman 2001; Duarte et al. 2012; Magistretti and Allaman 2015).

© The Author(s) 2019. Published by Oxford University Press.
This is an Open Access article distributed under the terms of the Creative Commons Attribution Non-Commercial License (http://creativecommons.org/licenses/by-nc/4.0/), which permits non-commercial re-use, distribution, and reproduction in any medium, provided the original work is properly cited. For commercial re-use, please contact journals.permissions@oup.com

Although these brain imaging techniques are suitable to characterize energy consumption associated with neuronal activity at the regional level, they cannot provide a cellular resolution. Over two decades of energy metabolism studies have provided evidence that astrocytes, a type of glial cells, play a major role in coupling neuronal activity to energy delivery (Magistretti and Allaman 2015). Astrocytes surround the endothelial cells and pericytes through specialized perivascular processes called end-feet and possess a large number of processes that ensheath synapses (Ventura and Harris 1999; Genoud et al. 2006; Calì et al. 2016). In fact, a single astrocyte can contact over 100000 synapses in the rodent brain (Oberheim et al. 2012).

From functional studies carried out ex vivo and in vivo, circulating glucose has been shown to be taken up during neuronal activity, predominantly by astrocytes which process it through aerobic glycolysis to produce lactate (Voutsinos-Porche et al. 2003; Chuquet et al. 2010). Such lactate is then transferred to neurons through specific monocarboxylate transporters (MCT) via a process known as the astrocyte–neuron lactate shuttle (ANLS) (Pellerin and Magistretti 1994, Magistretti and Allaman 2015; Magistretti and Allaman 2018; Calì et al. 2019).

Functional brain imaging techniques have also demonstrated aerobic glycolysis and subsequent lactate production during normal cerebral activation states (Fox et al. 1988; Raichle et al. 2006; Magistretti and Allaman 2015). Interestingly, a recent article (Hui et al. 2017) showed that circulating lactate in the blood stream is the preferential fuel of the tricarboxylic acid (TCA) cycle in all organs, as initially proposed for the brain, where the conversion of glucose to lactate entails an initial step taking place in astrocytes.

The role of lactate, synthesized from astrocytic glycolysis, has long been considered as solely providing an energy substrate, readily available for neurons (Pellerin and Magistretti 1994; Magistretti and Allaman 2015). Recent work has however extended the function of lactate as being a signaling molecule for neuronal plasticity. Indeed, the transfer of lactate from astrocytes to neurons is necessary for memory consolidation in several behavioral paradigms (Gibbs et al. 2006; Newman et al. 2011; Suzuki et al. 2011; Boury-Jamot et al. 2016), consistent with the induction by lactate of several plasticity genes in neurons (Yang et al. 2014; Margineanu et al. 2018). Furthermore, recent work showed how learning paradigms involving hippocampal CA1 result in increased lactate extracellular levels (Newman et al. 2017).

A source of lactate in the brain, in addition to glucose, is glycogen (Dringen and Hamprecht 1992), the storage form of glucose, which is exclusively localized in astrocytes (Nelson et al. 1968; Phelps 1972; Phelps 1975; Allaman et al. 2011).

In astrocytes, glycogen is mobilized by a restricted number of neurotransmitters such as vasoactive intestinal peptide (Magistretti et al. 1981) and noradrenaline (NA) (Magistretti et al. 1988), providing another example of neuron–glia metabolic coupling (Magistretti and Allaman 2015). Recently, the role of NA-evoked glycogenolysis in neuronal plasticity and memory consolidation has been demonstrated (Gao et al. 2016). This effect on astrocytes is mediated by beta-2 adrenergic receptors (β2r), and the ensuing c-AMP–mediated signaling cascade that promotes lactate production as a result of glycogenolysis (Sorg and Magistretti 1991).

The role of glycogen-derived lactate in plasticity and memory consolidation was demonstrated by showing that the pharmacological blockade of glycogenolysis by intrahippocampal injections of the glycogen phosphorylase (GP) inhibitor 1,4-dideoxy-1,4-imino-D-arabinitol (DAB) (Walls et al. 2008) resulted in amnesia following an inhibitory avoidance learning task, this amnesia being rescued by L-lactate (Suzuki et al. 2011). Similar observations were made in other learning tasks involving the prefrontal cortex and the basolateral amygdala (Gibbs et al. 2006; Newman et al. 2011; Boury-Jamot et al. 2016). Furthermore, blocking expression of astrocyte- and neuron-specific MCT (MCT 1, 4, and 2, respectively) resulting in inhibition of the transfer of lactate from astrocytes to neurons also resulted in amnesia. Lactate administration rescued the amnesia evoked by inhibition of the astrocyte-specific MCTs (MCT 1 and 4) but not that caused by inhibition of the neuron-specific transporter MCT2. Furthermore, the rescuing effect of lactate administration was not mimicked by glucose, thus indicating that lactate supports mechanisms other than energy supply (Suzuki et al. 2011, Vohra et al. 2019) in agreement with the observation that it induces expression of plasticity genes in neurons (Yang et al. 2014).

Long-term potentiation (LTP), which is generally considered an electrophysiological mechanism underlying memory formation, is also impaired by DAB and rescued by intrahippocampal lactate administration (Suzuki et al. 2011).

While this set of observations indicates a clear role of glycogen-derived lactate in plasticity gene expression and memory consolidation, the effects of lactate on synapse dynamic processes such as changes in surface, volume, and density that underlie plasticity and memory are unknown. In the present study, we provide direct evidence that lactate derived from glycogen in astrocytes is necessary for plasticity-induced structural changes in synaptic morphology following learning and in network dynamics evoked by LTP. This is demonstrated by both a 3D-electron microscopy characterization of hippocampal synapses and astrocytes and by the observation of organotypic slices in which LTP had been induced by carbachol-dependent theta bursts.

Methods

Animals

Male C57Bl/6 N mice (3 months old) were housed individually in polycarbonate cages, to avoid fights and aggressive behaviors that cause distress and potentially damage the cannulas implants. Food and water were freely available through wire lids. Cob-bedding were changed weekly, and the vivarium was kept at 21°C with a 12 hours' light cycle (lights on at 08:00). In order to mitigate the effects of isolation, each mouse was provided with enrichment material (tunnel tubes, climbing apparatuses, igloos). All the experimental procedures followed the guidelines established by the Italian Council on Animal Care and were approved by the Italian Government decree. All efforts were made to minimize the number of subjects used and their distress and suffering.

Surgery

Mice were anesthetized with intraperitoneal injection of chloral hydrate (450 mg/kg in a volume of 0.1 mL/10 g), which is known to not interfere with glycogen metabolism (Krieglstein and Stock 1973). Mice were then placed in a stereotaxic apparatus. The skin was incised, and the skull was cleaned. One 22-gauge guide cannula (2biological instruments S.N.C.) was placed 1 mm above the intended site of injection according to the atlas of

Downloaded from https://academic.oup.com/cercor/article-abstract/30/4/2114/5625994 by guest on 24 June 2020

Paxinos and Franklin (2001). Stereotaxic coordinates for the CA1 region of the dorsal hippocampus were anteroposterior: −2 mm from bregma, mediolateral (ML): ±1.9 mm from the sagittal suture, and dorsoventral (DV): −1.9 mm from the skull surface. The ± sign preceding the ML value indicates left and right direction from the center. The cannula was secured to anchor jewelers' screws with dental acrylic. A stainless steel stylet was inserted into the guide cannula to keep it free of debris. All animals were allowed 1 week to recover from surgery and to clear anesthetic. Control mice are mice that underwent only surgery for cannula implantation.

Drug Injection

For drug injection, the animals were gently restrained by hand; the stylet was removed from the guide cannula and replaced by injection needle (0.5 mm below the tip of the guide cannula). The injection solutions were administered in a total volume of 0.5 µL/(mouse × side) over a 60-second period through an infusion pump (KDS Model 100 KD Scientific Inc.). The injection needle was left in place for additional 60 seconds in order to facilitate the diffusion of the drugs. To verify the appropriateness of the coordinates of stereotactic injection site and procedure, 4 animals were injected with 0.5 µL of 0.4% Evans blue solution (E2129, Sigma-Aldrich). One hour after injection, the animals were sacrificed and the brain dissected, sectioned at the level of the dorsal hippocampus and directly imaged under a stereomicroscope (M205 FA Stereo Microscope Leica Microsystem). Mice were treated with the inhibitor of GP, DAB (D1542, Sigma-Aldrich), L-lactate (L7022, Sigma-Aldrich), or vehicle (artificial cerebrospinal fluid, aCSF). Injections into the hippocampus were made 15 minutes before the beginning of the tasks. When DAB was given in combination with L-lactate, one solution was prepared. The volume was 0.5 µL/(mouse × side). All the drugs were dissolved in aCSF prepared fresh (124 mM NaCl, 2.5 mM KCl, 2.0 mM $MgSO_4$, 1.25 mM KH_2PO_4, 26 mM $NaHCO_3$, 10 mM glucose, 4 mM sucrose, 2.5 mM $CaCl_2$). We injected bilaterally 0.5 mL/side of DAB (1000, 2000, and 4000 mM; 500, 1000, and 2000 pmol, respectively), 0.5 mL/side of vehicle (aCSF) or 0.5 mL/side of L-lactate 100 nmol.

Spontaneous Motor Activity

Spontaneous motor activity was evaluated using an automated activity cage (Ugo Basile) placed in a sound-attenuating room. Each system consists of an animal cage (43 × 43 × 32 cm) containing 16 photocells 3 cm above the floor under transparent cover, an electronic unit incorporating a counter and a printer. The rectangular animal cage has transparent sides and lid to allow for observations. The cage floor has horizontal and vertical infrared sensors. The counter sums up the photocell disruptions, and a printer displays the results at preset intervals. On the day of the test, each mouse was habituated to the room for 60 minutes in the home cage and then in the activity cage for 30 minutes. Cumulative horizontal beam breaks, every 5 minutes' interval period, during 30 minutes' observation period were counted.

Novel Object Recognition Test

Object recognition was conducted in an open plastic arena (38 cm × 30 cm × 18 cm). The apparatus is illuminated by a fluorescent lamp placed centrally above it (75 W). The animals were first habituated to the test apparatus for 10 minutes on Day 1 and then subjected to the familiarization trial (T1) and to a novel object recognition trial (T2). In order to study the DAB effect on long-term memory (LTM), we tested animals 24 hours after training. The total time spent exploring the two objects during T1 and T2 trial was taken as a measure of object exploration. To avoid the interference of olfactory cues, the sawdust was stirred and the objects were cleaned with 70% ethanol after each tested animal. The novel object was always changed at every delay time. The performance was evaluated by calculating a discrimination index $(N - F/N + F)$, where N = time spent exploring the new object (T2novel) during T2, F = time spent exploring the familiar object (T2familiar) during T2 (Fig. S2A).

Histological Analysis

Cannula placements were examined after behavioral testing to ensure correct placement. Mice were anesthetized by intraperitoneal injection of chloral hydrate (450 mg/kg in a volume of 0.1 mL/10 g) and transcardially perfused with 2% paraformaldehyde (19 200, Electron Microscopy Sciences) in phosphate-buffered solution 1 × (137 mM NaCl, 2.7 mM KCl, 10 mM Na_2HPO_4, 2 mM KH_2PO_4) pH 7.4. Dissected brains were further fixed in Bouin's fixative (Sigma-Aldrich) for 18–30 hours and then cleared and conserved in 70% (vol/vol) ethanol. Four transverse sections of each brain were obtained with an adult mouse brain matrix and processed together. Samples were processed using an automated tissue processor (ASP300, Leica Microsystem) and paraffin embedded. Briefly, samples were rinsed in bidistilled water for 30 minutes, then were gradually dehydrated through an ethanol (02860, Sigma-Aldrich) series (50%, 70%, 90%, 100%) and xylene (95 672, Sigma-Aldrich) at room temperature (RT) and finally embedded in paraffin (327 212, Sigma-Aldrich) at 62°C. Blocks were cut in 8–15 mm sections with a microtome (RM 2255, Leica Biosystems, Nussloch GmbH).

Hematoxylin and Eosin Staining

Sections were stained with hematoxylin and eosin (Diapath S.p.A.) and studied under a light microscope (Leica DM750, Leica Microsystem). The sections were deparaffinized in xylene and rehydrated, at room temperature, through a decreasing ethanol series (100%, 95%, and 70%) and rinsed in bidistilled water. The staining consisted in the incubation of sections in hematoxylin for 3 minutes, in the rinsing in running water for 5 minutes and then in the counter-staining with eosin for 3 minutes. Sections were subsequently dehydrated with an increasing ethanol series (95% and 100%) and xylene and mounted with Micromount mounting medium (060200, Diapath S.p.A). Histological sections were visualized with an optical microscope (DM 2500, Leica Microsystem) and acquired with a digital camera (DFC310FX, Leica Microsystem) associated with the Leica Image Manager Software.

Golgi-Cox Staining

Twenty-four hours after the training, and immediately after the behavioral session, mice (at least 3 for each group) were anesthetized by intraperitoneal injection of chloral hydrate (450 mg/kg in a volume of 0.1 mL/10 g) and transcardially perfused with 15 mL of saline solution (0.9% NaCl). After perfusion, dissected brains were quickly immersed in Golgi-Cox solution (potassium dichromate 1%, mercuric chloride 1%, and

Downloaded from https://academic.oup.com/cercor/article-abstract/30/4/2114/5625994 by guest on 24 June 2020

potassium chromate 0.8%) (AnalaR B.D.H.) and stored at room temperature for at least 6 days in the dark. After this period of impregnation, brains were washed in water several times to remove the excess Golgi-Cox solution and incubated in a 30% sucrose (Sigma-Aldrich) solution for at least 2 days in the dark at 4°C. One hundred µm coronal sections were obtained with a vibratome (Leica VT1000S) and were mounted on gelatine-coated glass slides (2% gelatine, 1% KCr $(SO_4)_2$ 12 H_2O). After 24 hours, brain slices were treated in the dark as follows: slices were washed twice with water and incubated for 30 minutes in ammonium hydroxide (05002, Sigma-Aldrich) at RT. Rinsed slides were fixed for 30 minutes in Kodak fix solution (P8307, Sigma-Aldrich). Subsequently slices were dehydrated with an ethanol series (50%, 70%, 95%, and 100%) for 5 minutes each, then a solution composed by 1/3 chloroform, 1/3 xylene, and 1/3 ethanol for 15 minutes and xylene (185 566, Sigma-Aldrich) for 15 minutes. Sections were subsequently mounted with a coverslip using Micromount mounting medium.

Image Acquisition and Quantitative Analyses

Stained neurons from the CA1 region of hippocampus were acquired using an Axiovert 200 M (Carl Zeiss) spinning disc confocal system (PerkinElmer Life Sciences Waltham). Stacks were collected every 0.5 µm with a 20 ×, 40 × (oil), and 63 × (oil) objective. Ten pyramidal neurons from the DV hippocampal CA1 (*stratum radiatum*) were studied from three animals for each group (20 dendritic shafts and at least 1300 µm of dendrites per group were analyzed). Pyramidal neurons from the *stratum radiatum* of hippocampal CA1 were studied because in this region, the CA3-proceeding Schaffer collaterals synapse with dendritic spines from the dendritic arborization of pyramidal cells, mostly in the *stratum radiatum*. The spine density of the proximal apical dendrite area was analyzed (minimum 100 µm from soma), the second- or third order of dendrite (protruding from its parent apical dendrite) was chosen for spine density quantification. Z-stacks were made from each dendrite in the whole of the analyzed segment. To determine the spine density, ImageJ1.47v software (National Institute of Health) was used.

Serial Block-Face Electron Microscopy

Twenty-four hours after the training, and immediately after the behavioral session, mice (2 controls and 3 for all other groups) were deeply anesthetized by intraperitoneal injection of chloral hydrate (450 mg/kg in a volume of 0.1 mL/10 g) and transcardially perfused with 2.5% glutaraldehyde (16 220, Electron Microscopy Sciences Hatfield), 2% paraformaldehyde in 0.15 M sodium cacodylate buffer (12 300, Electron Microscopy Sciences Hatfield). Coronal sections (100 µm thickness) were obtained by vibratome (Leica VT1000S), and hippocampi were manually dissected from these sections. After washing by cold cacodylate buffer 0.1 M, samples were fixed in a reduced osmium solution containing 3% potassium ferrocyanide (P3289, Sigma-Aldrich) in 0.3 M cacodylate buffer combined with an equal volume of 4% aqueous osmium tetroxide, for 1 hour, on ice. At the end of the first heavy metal incubation, the tissues were washed with bidistilled water at RT and then were placed in the 0.22 m-Millipore-filtered 1% thiocarbohydrazide (88 535, Sigma-Aldrich) in bidistilled water solution for 20 minutes, at RT. Tissues were then rinsed again in pure bidistilled water and incubated in 2% osmium tetroxide water solution in for 30 minutes at RT. After several washings at RT in bidistilled water, they are then placed in 1% uranyl acetate (aqueous), and left overnight at 4°C. Samples were then washed again, to be immersed en-bloc in Walton's lead aspartate solution (0.066 g lead nitrate dissolved in 10 mL of 0.003 M aspartic acid solution, pH 5.5) (228 621 and A9256, Sigma-Aldrich) at 60°C for 30 minutes. The tissues were washed once again and dehydrated using ice-cold solutions of freshly prepared ethanol series, then placed in anhydrous ice-cold acetone (650 501, Sigma-Aldrich) for 10 minutes and embedded in Durcupan resin (44610-1EA, Sigma-Aldrich) cured at 60°C for 48 hours. Resin blocs were mounted on aluminium specimen pins (10-006002-10, Micro to Nano) using cyan acrylic glue and trimmed with a glass knife to a rectangle 0.5 × 0.75 mm, with the tissue exposed on all four sides. Silver paint (16 062—PELCO Conductive Silver Pain, TedPella) was used to electrically ground the edges of the tissue block to the aluminium pin. The entire specimen was then sputter coated with a thin (25 nm) layer of gold (High Resolution Cressington Sputter Coater 208 HR sputter coater, TedPella Inc.).

3D Reconstructions and Analyses

Serial block-face images are collected using a Gatan 3View system (Gatan) mounted in an FEI Quanta FEG 200 SEM operating at an acceleration voltage of 3 kV with an in-chamber pressure of 10 Pa of water vapor. Samples were imaged at 10 000 × in order to visualize dendritic spines and PSD; the voxel size is 6 × 6 × 50 nm (x-y-z), the latter was chosen as the thickness for the SEM cutting interval. The resulting datasets were assembled into aligned volume files using Digital Micrograph (Gatan) and then semiautomatically or manually segmented and reconstructed in 3D using Ilastik 0.5 or 1.2 (www.ilastik.org) or AMIRA 5.4.3 software package (FEI Visualization Science Group), respectively. 3D models were either measured using the "Material Statistics" module of AMIRA, or Neuromorph addon available for Blender (www.blender.org).

Slice Cultures and Transfections

Transverse hippocampal organotypic slice cultures of 400-µm-thick were prepared from 7-day-old rats as previously described (De Roo et al. 2008b; De Roo and Ribicic 2017), using a protocol approved by the Geneva Veterinarian Office (authorization 31.1.1007/3129/0). Slice cultures were maintained for 16 days on small membrane confetti placed on top of Millipore insert in a CO_2 incubator at 33°C. Slice cultures were allowed to recover for 7 days before transfection was done with a pCX-mRFP plasmid using a biolistic method (Helios Gene Gun, Bio-Rad). The first imaging session occurred at day in vitro 11.

Confocal Imaging

Laser scanning microscopy was done with a Fluoview 300 system (Olympus) as previously described. In brief, transfected slice cultures were immersed with culture medium for short imaging period (<10 min) in a temperature-controlled recording chamber (28°C), then transferred back to the incubator. A dendritic segment of 35 µm in length and located between 100 and 200 µm from the soma of CA1 pyramidal neurons (one segment per cell and per experiment) was imaged in 3D with a 40 × objective using a 10 × additional zoom (final definition, 25 pixels/µm; z-step between scans, 0.4 µm). A 3D image (3 µm z-step) of the neuron was performed the first and last imaging day using a 40 × 0.80 NA objective (Olympus) in order identify pyramidal neuron

Downloaded from https://academic.oup.com/cercor/article-abstract/30/4/2114/5625994 by guest on 24 June 2020

and check overall neuron health. Neurons remained healthy and fluorescence remained stable during the whole experiment duration and they could be imaged for longer if desired (De Roo et al. 2009). Dendritic spine turnover and survival analysis were performed blind on z stacks of raw images using a home-made plugin for OsiriX software (http://www.osirix-viewer.com). Spine width was measured using the maximum diameter of the spine head on individual z-images. Situations that did not allow a precise spine head width measurement (two spine heads overlapping each other on the same z sections) were excluded. Due to the known lack of stabilization of filopodia on several days, stability analysis was carried only on dendritic spines.

Drug Incubation for Experiments in Organotypic Cultures

DAB, Carbachol, and L-lactate (Sigma-Aldrich) were added in the culture medium after the first imaging session. DAB with or without L-lactate was added immediately and washed out after 90 minutes of incubation. Carbachol was added after 30 minutes and washed out after 1 hour of incubation.

Statistical Analyses

Results were statistically analyzed by GraphPad Prism version 6 and 8 (GraphPad Software). All data are presented as mean ± SEM. *N* indicates number of animals. Comparisons of distribution data between two groups were analyzed by Kolmogorov–Smirnov test. Multiple group comparisons were assessed using a one-way analysis of variance, followed by the post-hoc Tukey-multiple comparison test. Means were considered statistically different when $P < 0.05$. For confocal imaging, all statistics are given with the standard error of the mean. Normality was tested for each distribution (D'Agostino and Pearson test), and alpha was set to 5% for all tests.

Results

DAB induces amnesia and prevents hippocampal spine density increase following learning, both effects being rescued by L-lactate.

Glycogenolysis and astrocytic lactate release are critical for synaptic plasticity, long-term memory and its underlying molecular and synaptic changes (Suzuki et al. 2011). By taking a similar approach used in Suzuki et al. 2011, we tested memory performance 24 hours after novel object recognition (NOR; Fig. 1A) training in mice. In order to determine a minimally effective dose of DAB, we performed a dose–response experiment to obtain long-term memory inhibition, regardless of previous experiments in rats. C57BL/6 N mice received bilateral intrahippocampal injections of DAB at three different concentrations (500 pmol, 1000 pmol, and 2000 pmol), vehicle (control conditions), or DAB together with 100 nmol L-lactate, 15 minutes before the training phase (Fig. 1A). In control experiments, Evans blue bilateral intrahippocampal injections showed the correct diffusion of the drug in the hippocampus (Fig. S1A). Histological analyses of coronal brain sections confirmed that the tip of the injection cannula reached the dorsal hippocampus (Fig. S1B); moreover, no changes were revealed in the spontaneous motor activity after DAB injection (Fig. S2B).

Mice injected with 1000 pmol and 2000 pmol DAB failed to exhibit LTM formation, in contrast to what was observed with vehicle- or 500 pmol DAB-injected mice (Fig. 1B). Therefore, we used 1000 pmol DAB for all further investigations, as this was the minimal effective dose. Mice coinjected with 1000 pmol DAB and 100 nmol L-lactate (Fig. 1B) displayed normal memory, indicating a rescue effect by L-lactate.

The observed difference in the effective DAB concentration between mice (the present study, 1000 pmol) and rats (Suzuki et al. 2011, 300 pmol) could be due to the rate of metabolism of a particular drug that may vary considerably in different animal species. Generally, mice need higher drug doses than rats since their metabolism is faster (Sakai et al. 2014).

To investigate whether memory impairment correlates with structural changes in the hippocampi of DAB-treated mice, we quantified spines on proximal dendrites of pyramidal neurons.

Golgi staining (Fig. 1C–E) revealed that learning induced a 10% increase in the linear density of spines in vehicle-treated mice (Fig. 1F), in agreement with previous reports exploiting the same learning task (Menna et al. 2013). Spine density increase was inhibited by DAB and rescued by coapplication of DAB with L-lactate (Fig. 1F). Finally, the injection of the sole vehicle, i.e., the aCSF, did not give raise to any change in the linear spine density of mice not performing a learning task, as shown in Figure S3 and corresponding Table S4.

DAB blockade of the LTP-dependent increase in spine formation and stabilization are rescued by L-lactate.

We next investigated whether lactate derived from astrocytic glycogen plays a role in plasticity-related spine dynamics using an in vitro model of LTP in hippocampal organotypic slice culture. Organotypic hippocampal slices have been advantageously used to study plasticity mechanisms following induction of LTP, in particular in terms of spine density and dynamics (De Roo et al. 2008a; Oe et al. 2013). Specifically, LTP stabilizes the mushroom type spines in hippocampal slices within 2 hours (Sorra and Harris 1998; Bourne and Harris 2011) and increases spine density, 24 hours after induction, an effect that is maintained over weeks (Oe et al. 2013). LTP was induced by carbachol (Cch) application at 10 µmol for 1 hour as previously described (De Roo et al. 2008a; Oe et al. 2013). Individual spine dynamics of CA1 pyramidal neurons was imaged over 24 hours (Fig. 2A). Cch in organotypic slices induces theta-bursts, a learning-related pattern of activity in vivo, which increases the presence of polyribosomes in enlarged spines, an evidence for a rapid and sustained induction of protein synthesis in stable spines (Bourne and Harris 2011). As previously shown (De Roo et al. 2008a), Cch increased the percentage of spine turnover over 24 hours (formation and elimination; Fig. 2B,C) and consequently decreased the stability of individual spines (Fig. 2D,E). DAB at 300 µmol in the presence of Cch impaired the formation of new spines (Fig. 2C) exclusively, correlating well with the effect observed in vivo (Fig. 1F). Incubation of DAB together with L-lactate (5 mmol, 90 minutes) rescued the activity-dependent increase in spine formation (Fig. 2C) and its dynamics (Fig. 2E). Note that in the absence of Cch neither L-lactate nor DAB alone affected spine dynamics (Fig. S4A-C) nor the selective stabilization of head-enlarging mushroom spines (Fig. S5A, B).

L-lactate rescues DAB-inhibited formation of new spines but not spine and PSD size.

We then quantified the ultrastructural features related to memory formation, and their DAB-dependent impairment, using a 3D-EM approach, by measuring the 3D-reconstructed spine density (Fig. 3A,B), spine head, and PSD surface area (Fig. 3C,D).

Analysis of spine density in hippocampal volumes (513.8 μm^3/mouse, Fig. 3A) prepared from mice that underwent NOR matched the observations made on linear densities using Golgi stain (Fig. 1F) ruling out possible tissue shrinkage artifacts. Spine

Downloaded from https://academic.oup.com/cercor/article-abstract/30/4/2114/5625994 by guest on 24 June 2020

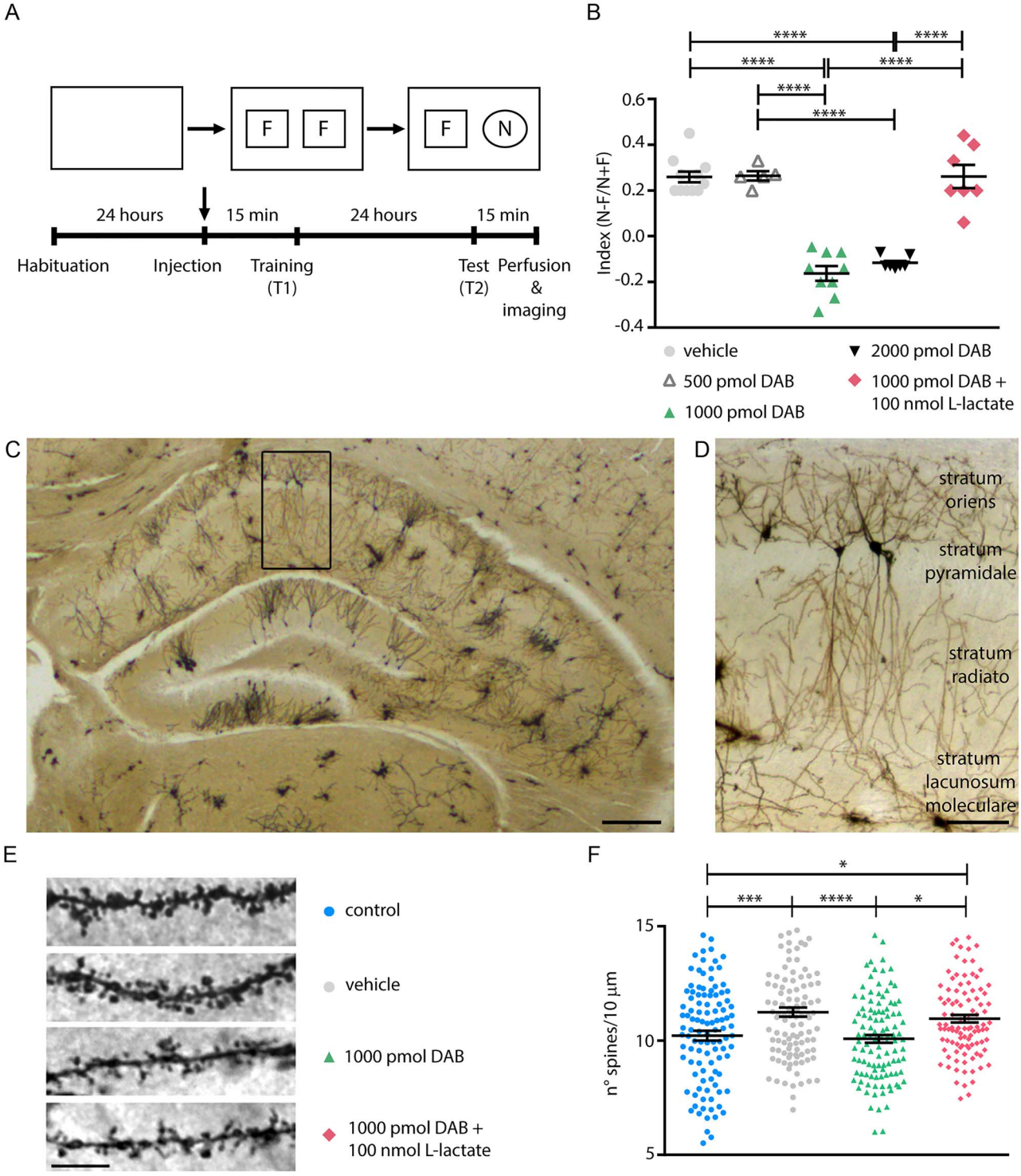

Figure 1. L-lactate rescues amnesia and hippocampal spine density impaired by DAB. (*A*) Schematic of the NOR experimental protocol. (*B*) Memory impairment was present in mice injected with 1000 and 2000 pmol DAB and administration of 100 nmol L-lactate in combination with 1000 pmol DAB, rescues amnesia in the NOR test. (*C*), (*D*) Images of 100 µm coronal section stained according to the Golgi-cox method. Scale bars, 300 µm and 100 µm. (*E*) Representative examples of Golgi-stained hippocampal neurons showing apical dendritic segments at high magnifications to highlight dendritic spines in mice control, injected with vehicle, 1000 pmol DAB, and 1000 pmol DAB +100 nmol L-lactate (scale bar: 10 µm). (*F*) Quantitation of spine number per 10 µm dendritic segment 24 hours from NOR training. (*B*), (*F*) $^{*}P < 0.05$, $^{**}P < 0.01$, $^{***}P < 0.001$, $^{****}P < 0.0001$ one-way analysis of variance, Tukey's test (see Table S1).

Downloaded from https://academic.oup.com/cercor/article-abstract/30/4/2114/5625994 by guest on 24 June 2020

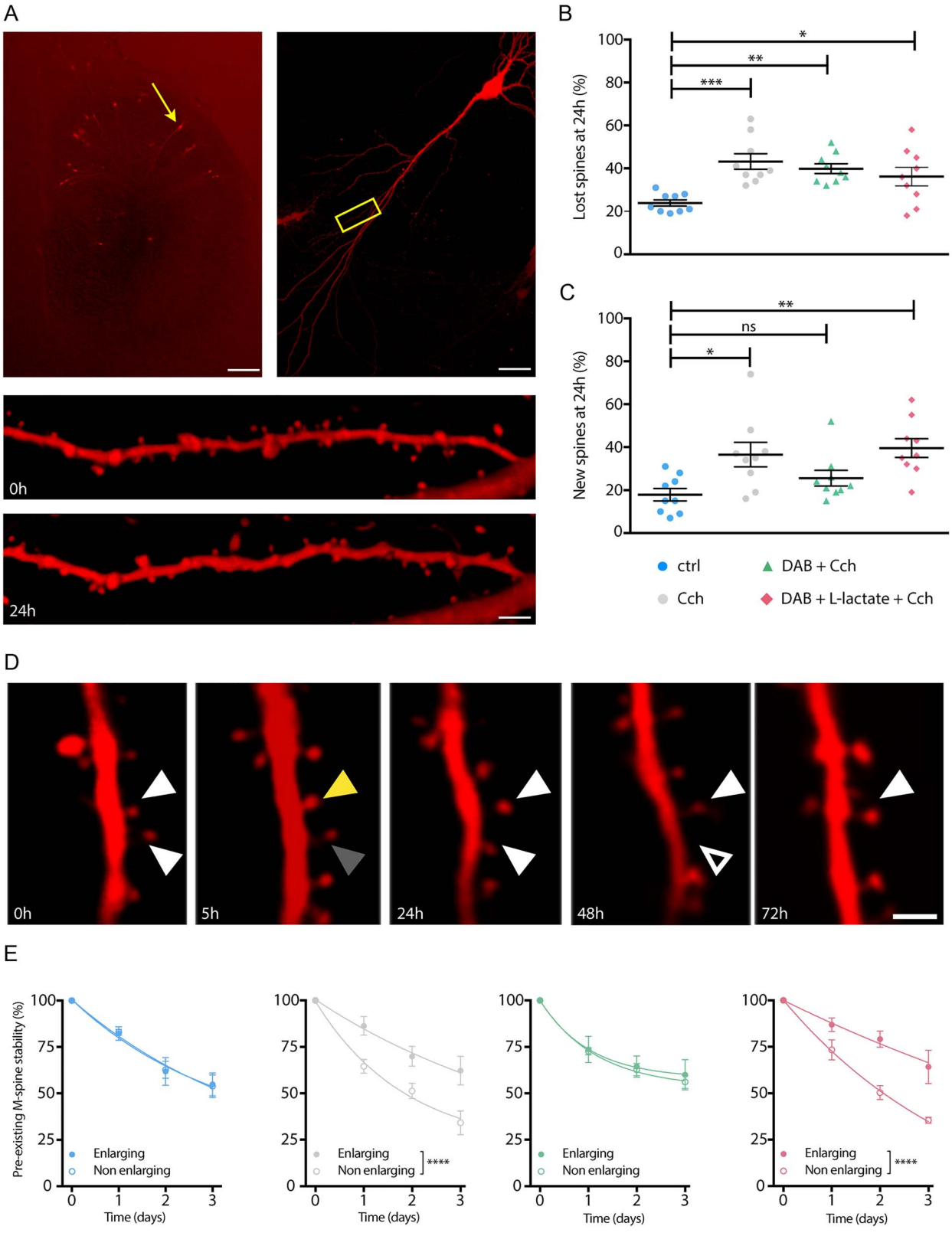

Figure 2. DAB blockade of the LTP-dependent increase in spine formation and stabilization are rescued by L-lactate. (*A*) Individual spines on dendritic segments are imaged in transfected CA1 hippocampal pyramidal neurons. (*B*) Cch increased the percentage of eliminated spines (lost spines) at 24 hours after inducing of LTP in all experimental conditions. (*C*) Cch-induced LTP increase of the percentage of new spines after 24 hours was blocked with DAB and rescued by L-lactate. (*D*) Preexisting individual spines (left, white arrowhead) were either enlarging at 5 hours and stabilized over 4 days (yellow arrowhead) or nonenlarging at 5 hours (gray arrowhead). (*E*) Cch-induced selective spine stabilization was blocked by DAB and rescued by L-lactate. $^{*}P < 0.05$, $^{**}P < 0.01$, $^{***}P < 0.001$, $^{****}P < 0.0001$. (*B*), (*C*) One-way analysis of variance, Kruskal-Wallis test. (*E*) Two-way analysis of variance. Scale bars: (*A*) left: 500 µm, right: 50 µm, bottom: 4 µm, (*D*) 2 µm (see Table S2).

Downloaded from https://academic.oup.com/cercor/article-abstract/30/4/2114/5625994 by guest on 24 June 2020

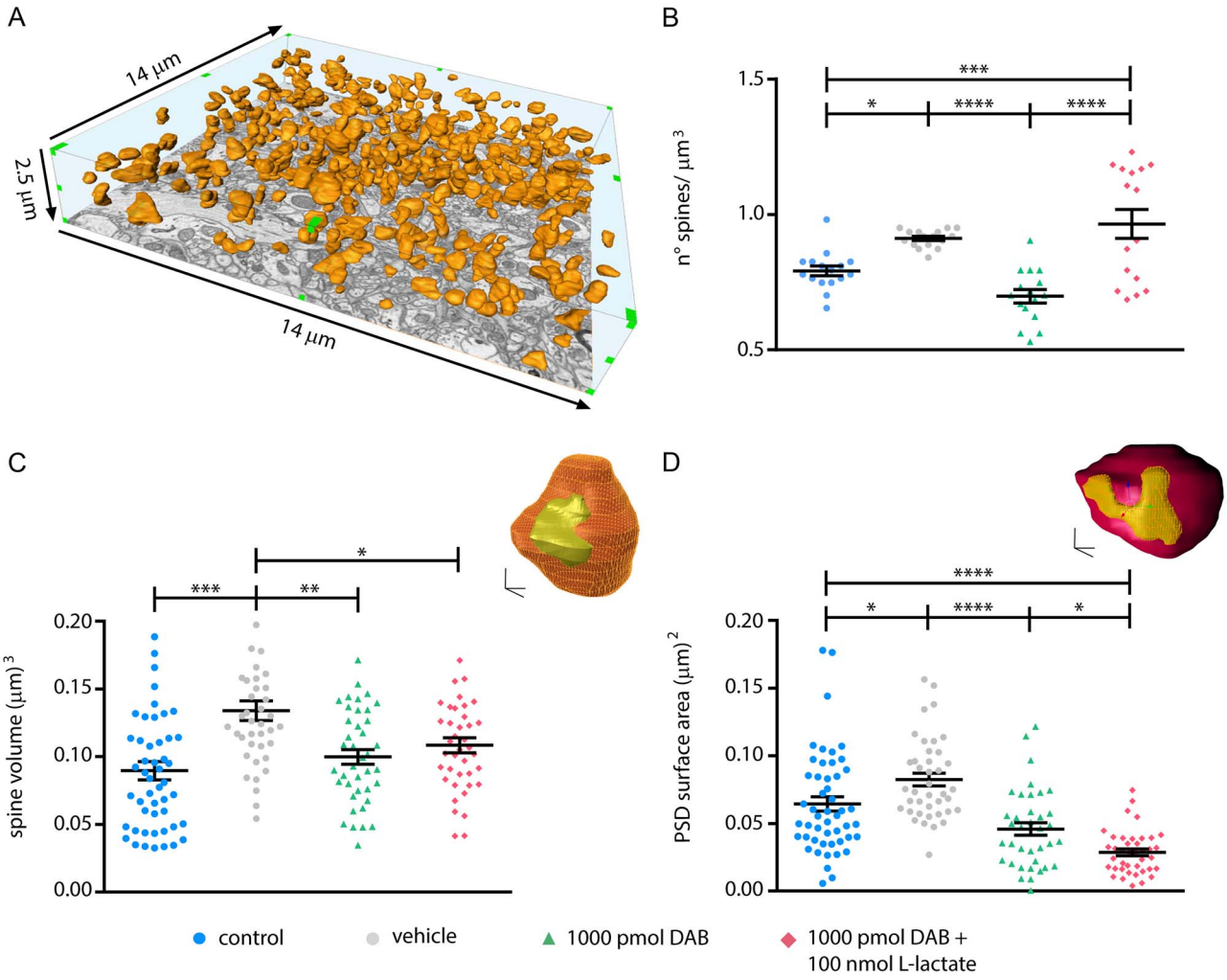

Figure 3. L-lactate rescues DAB-inhibited formation of new spines but not spine and PSD size. (A) Example of three-dimensional reconstruction of dendritic spines heads (orange) in a hippocampal CA1 volume of 513.8 µm^3. (B) DAB treatment significantly reduced the spine density 24 hours after NOR training and 100 nmol L-lactate coinjected with 1000 pmol DAB rescues the spine density. (C) 3D reconstruction of a spine head (orange) with its PSD (yellow); 3D-scale bar: 200 nm. Graph represent spine size measured with Blender, note the increase of the spine volume after learning (control vs. vehicle) and the decrease after DAB injection that is not rescued by L-lactate. (D) 3D reconstruction of a spine head (purple) with its PSD (yellow); 3D-scale bar: 200 nm. Graph represent PSD size measured with Blender, note the increase of the PSD size after learning (control vs. vehicle) and the decrease after DAB injection that is not rescued by L-lactate. (B), (C), (D) *$P < 0.05$, **$P < 0.01$, ***$P < 0.001$, ****$P < 0.0001$; one-way analysis of variance, Tukey's test (see Table S1).

density in vehicle-treated mice increased by 15% after learning compared to naive (control) mice. DAB treatment prevented the spine density increase, while the concomitant administration of DAB and L-lactate completely rescued it (Fig. 3B) resulting in an increase up to 21% compared to control. In line with results in organotypic slices (Fig. 2B,C), the density increase of spines 24 hours after learning is due to the insertion of new stable spines (Fig. 2E), which is prevented by DAB.

We also extended our 3D analysis of postsynaptic structural reorganization to two other levels: dendritic spine size and PSD surface area. We observed that DAB indeed inhibited these two elements of learning-induced plasticity. Interestingly, this inhibitory effect was not rescued by L-lactate coinjection with DAB (Fig. 3C,D).

Thus, hippocampal synapses in control NOR-trained mice showed a 44% increase (Fig. 3C) in spine volume and 28% increase in PSD surface area (Fig. 3D). DAB inhibited these increases; coadministration of 100 nmol of L-lactate with 1000 pmol DAB, a combination that rescued the behavioral phenotype, failed to rescue the inhibition by DAB of spine volume and PSD surface area increases evoked by learning (Fig. 3C,D).

Only a few reports have described an increase in the size of the newly-formed spines during hippocampal LTP in slices (De Roo et al. 2008a; Bell et al. 2014), an effect believed to be associated with synaptic stabilization following plasticity. Altogether, results from the present study indicate that preventing lactate production by astrocytes does not affect basal spine turnover but does indeed prevent the formation of new spines and the finely selective preexisting spine stabilization triggered by LTP in the theta/gamma range.

Glycogen accumulation correlates with spine stabilization and learning.

Finally, we tested how DAB affected the astrocytic glycogen content under the various conditions examined in this study. We used the average diameter of glycogen granules, easily

Downloaded from https://academic.oup.com/cercor/article-abstract/30/4/2114/5625994 by guest on 24 June 2020

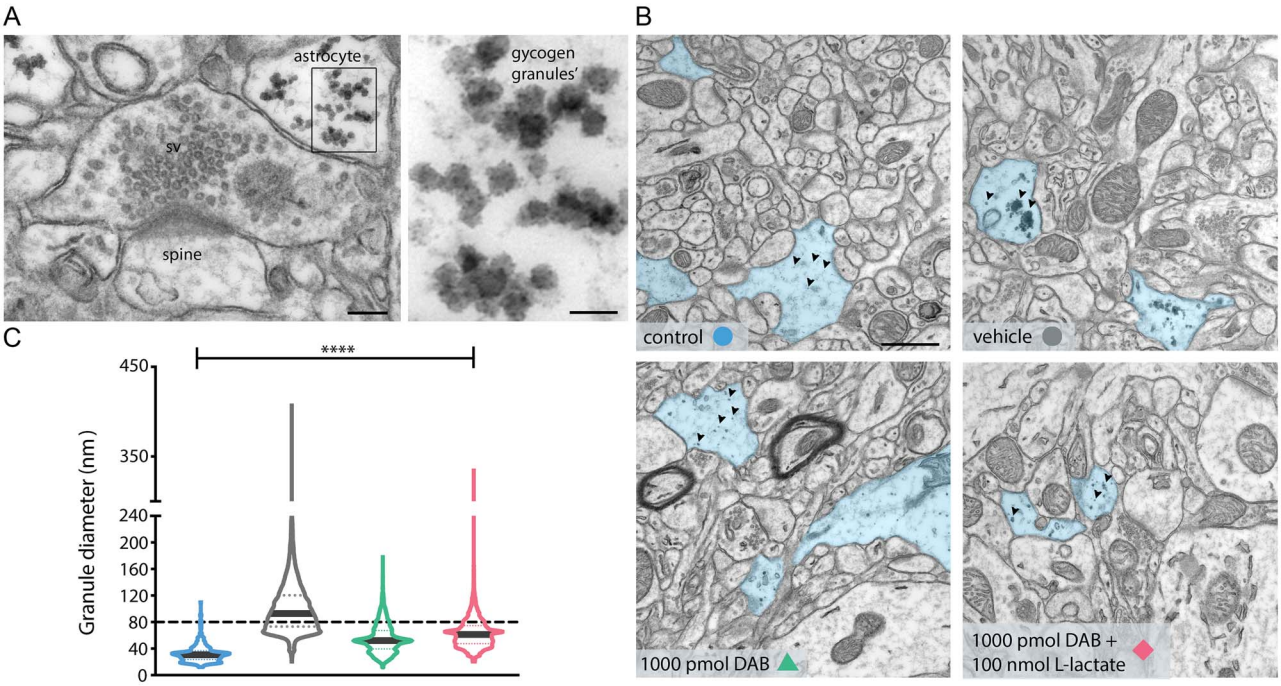

Figure 4. L-lactate does not rescue DAB-inhibited glycogen resynthesis. (A) TEM image of hippocampal excitatory synapses of mice treated with vehicle 24 hours after NOR training. In the astrocytic process contacting the presynaptic terminal, the glycogen granules are clearly visible, and the magnification shows the single granules inside the astrocyte. Scale bars: 100 nm and 50 nm. (B) Electron micrographs showing an increase of 221% in glycogen clusters' size after learning in mice treated with vehicle versus control mice, and inhibitory effect of 1000 pmol DAB on glycogen granules' resynthesis after learning that it is not rescued by L-lactate coadministration. Astrocytes processes are highlighted in blue and arrowheads indicated the glycogen granules'. Scale bar: 1 µm. (C) Corresponding violin plot of glycogen granules diameter. ****$P < 0.0001$; one-way analysis of variance, Tukey's test (see Table S1).

distinguishable as electron-dense granules (Fig. 4A) within astrocytic profiles, as a measure for their dynamics. Following learning, the size of astrocytic glycogen granules increased drastically (+221%; Fig. 4B,C) compared to control, where basal levels were almost undetectable. Pretreatment with 1000 pmol DAB blocked the increase in glycogen granule size versus control (Fig. 4B,C), while coadministration of 100 nmol of L-lactate with 1000 pmol DAB, a combination that rescued the behavioral phenotype of the mice, failed to rescue the decrease of the glycogen granules size (Fig. 4B,C). Granules clustering was also affected as density of glycogen granules per volume of astrocyte, which increased in learning mice (vehicle, 25.7 ± 2.7 granules/µm^3) compared to untrained mice (control, 8.2 ± 2.1 granules/µm^3). In the DAB treated (DAB, 11.2 ± 2 granules/µm^3) or rescue group (DAB + L-lactate, 15.1 ± 4.4 granules/µm^3), no change in density of glycogen granules was noted. This observation is not surprising since lactate is not a substrate for glycogen granule resynthesis, but rather a product of glycogenolysis.

Discussion

Previous work showed that glycogen-derived L-lactate and its transfer from astrocytes to neurons is necessary for memory consolidation (Gibbs et al. 2006; Newman et al. 2011; Suzuki et al. 2011). The use of DAB, a potent inhibitor of GP that also affects glycogen synthase (Walls et al. 2008), has been shown to inhibit the extracellular release of L-lactate. Besides its role as energy substrate, L-lactate is a key element in the formation of long-term memory by increasing the expression of transcription factors such as ARC, c-FOS, and ZIF 268 (Yang et al. 2014; Margineanu et al. 2018). This effect is mediated through the positive modulation by L-lactate of NMDA receptor-dependent signaling (Yang et al. 2014).

The main aim of the present study was to investigate how learning and memory consolidation modify the ultrastructure of the hippocampal neuropil, and whether and how these modifications could be influenced by neuroenergetic changes, in a NOR behavioral training. The hippocampus is considered an important neuroanatomical substrate for novel object recognition (Mumby 2001), particularly in the maintenance of strong, novel object preference after long delays (Hammond et al. 2004). Here, we observed that memory formation is associated with an increase in dendritic spine density in situ 24 hours after training. Interestingly, we also imaged a postsynaptic structural reorganization in terms of dendritic spine density and size, and PSD surface area. Importantly, linear spine density analysis performed on Golgi stained sections matched the results obtained with 3D-EM volume analysis.

Dendritic spines are the primary site of excitatory input on most principal neurons and are essential for functional synaptic plasticity and cognitive function. Accordingly, alterations in spine shape, size, and number induce long-lasting changes in synaptic activity and cognitive function (Muller et al. 2000; Lamprecht and LeDoux 2004). Furthermore, dysfunctional dendritic morphology is often correlated with neurological disorders characterized by abnormalities in cognition, emotion, and memory function.

The dynamics of spine formation following LTP is fairly complex. Expected changes might not appear shortly (minutes to

Downloaded from https://academic.oup.com/cercor/article-abstract/30/4/2114/5625994 by guest on 24 June 2020

a few hours) after the induction of LTP, although LTP has been shown to stabilize within 6 hours the mushroom-type spines in hippocampal slices (Sorra and Harris 1998; Bourne and Harris 2011). LTP assays *in vivo* (Medvedev et al. 2010; Medvedev et al. 2014), as well as in preparations that maintain circuit integrity such as organotypic hippocampal slices (De Roo et al. 2008a; Oe et al. 2013), have shown similar results, and a long-lasting stabilization of active spines, *i.e.,* over weeks (Oe et al. 2013). Moreover, LTP induced an increase of spine density 24 hours after its induction (Oe et al. 2013).

We observed that LTP in organotypic slices promoted by Cch-induced theta bursts, caused a general increase in spine turnover, with an increase in the ratio between enlarging, stabilizing spines, and smaller spines. A few observations have reported an increase in the size of the newly formed spines during hippocampal LTP in slices (Bourne and Harris 2011; Bell et al. 2014), an effect believed to be associated with synaptic stabilization following plasticity. Theta-burst stimulation in CA1 increases the presence of polyribosomes in enlarged spines within 5 minutes after stimulation of the effect being persistent 2 hours after the induction of LTP. This suggests a rapid and stable induction of protein synthesis in stable spines (Bourne and Harris 2011), a likely energy consuming process. A similar effect has been reported in situ, where LTP induced on awake rats increased the proportion of mushroom spines after 24 hours (Medvedev et al. 2010). Therefore, mushroom spines are considered to be stable "memory spines" (Bourne and Harris 2007). Furthermore, previous studies suggested that dendritic spine density is associated with cognitive ability (Leuner and Shors 2004).

Consistent with these observations on spine dynamics, in the present study, we observed a 50% increase in average spine volume size following learning that was impaired after DAB injection. Size increase of the dendritic spines correlated well with the increase in the PSD surface area following learning. Indeed, the size of the PSD has been shown to correlate with the spine size in basal conditions (Calì et al. 2018), although the increase in PSD surface area correlates with the so-called "nascent zones" adjacent to the active part of PSD, which might receive membrane from the recycling pool of the facing presynaptic terminal (Bell et al. 2014).

Glycogen is visible inside astrocytic processes using electron microscopy images as electron-dense, spherical granules (Phelps 1972; Phelps 1975; Takado et al. 2015a; Takado et al. 2015b; Calì et al. 2016). Since qualitatively an effect on glycogen granules was evident at the EM level, we further proceeded with a quantitative analysis. Using an automated reconstruction pipeline (Sommer et al. 2011), we could quantitatively determine that learning induced formation of clusters, largely over 80 nm diameter, which is considered to be the limit size for single alpha particles (Marchand et al. 2002). Learning induced a marked increase in the size of glycogen granules measured 24 hours after training (+221%) compared to control, nonlearning animals, in which basal levels of glycogen are low (Fig. 5), suggesting that energy stores in astrocytes are modulated by learning.

From a teleological point of view what was observed would suggest that mechanisms activated during learning and plasticity establish a novel regime for glycogen metabolism that aims at ensuring adequate energy reserves and supply to maintain in a stabilized state the synapses in the network engaged in learning. Mechanistically, activation of the astrocytic β2-adrenergic receptors, a strong signal for glycogenolysis (Magistretti et al. 1981) in astrocytes, is necessary for contextual

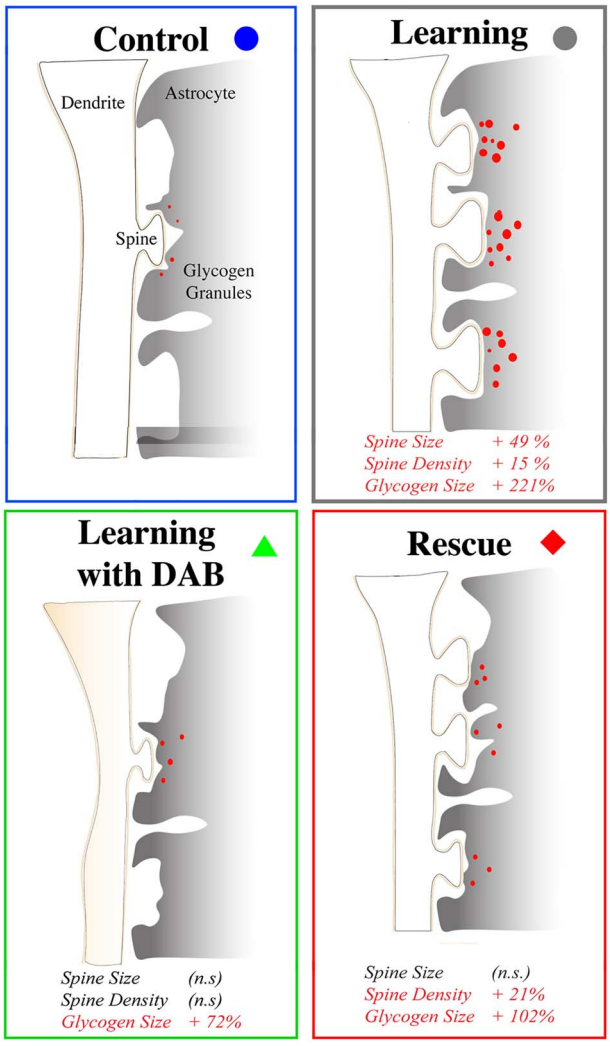

Figure 5. Schematics of the structural effects of LTP, its impairments by DAB and its rescue by L-lactate.

memory stabilization (Gao et al. 2016). Thus, learning and the associated coeruleo-cortical noradrenergic activation would result first in glycogenolysis and the ensuing lactate release from astrocytes, followed by a massive glycogen resynthesis, which we observed in this study. This sequence of noradrenergically triggered events has been described in vitro in primary astrocyte cultures (Sorg and Magistretti 1991) and involves the induction of the C/EBP family of transcription factors (Cardinaux and Magistretti 1996) and of Protein Targeting to Glycogen, an enzyme that turns glycogen metabolism toward a glycogen-synthesizing mode (Allaman et al. 2000).

Altogether, this set of data indicate that LTM and in vitro LTP result in an increase in the number of spines at 24 hours after learning and LTP induction, respectively. In vitro experiments suggest that both the insertion of larger spines and the removal of smaller ones occurs, a fact that is consistent with the average larger spine size observed at the ultrastructural level in hippocampus of mice that underwent the NOR learning protocol. Suzuki et al. (2011) previously showed the role of glycogen and L-lactate in both LTM and LTP. More recently, the role of L-lactate transfer from astrocytes to neurons in memory consolidation

Downloaded from https://academic.oup.com/cercor/article-abstract/30/4/2114/5625994 by guest on 24 June 2020

in the NOR test in rats has been demonstrated (Korol et al. 2019) by specifically blocking the neuronal MCT2 using alpha-cyano-4-hydroxycinnamate (4-CIN) in the dorsal hippocampus. In accordance with these results, we show that a single intrahippocampal injection of DAB, 15 minutes before the NOR training session, is sufficient to induce amnesia in mice tested for long-term memory 24 hours later. The behavioral phenotype was rescued by coinjecting in the dorsal hippocampus L-lactate, which bypasses the impaired glycogen-dependent ANLS.

Since DAB is known to have a direct effect on glycogen turnover, which is in turn associated to learning and synaptic reorganization, we have investigated the effects of the inhibition of glycogenolysis on all the structural rearrangements observed previously, following learning and LTP. Postsynaptic structural reorganization in terms of dendritic spine density, size, and PSD size was inhibited by DAB. The effects observed on the spines could be explained by the observations on spine dynamics in organotypic slices, where DAB exposure had an impact only on the new spines after 24 hours, but not on the eliminated spines. Indeed, the theta-burst primes a process that increases the turnover of spines, and in particular the removal of smaller spines to favor the stabilization, and possibly the growth of more mature spines. One could speculate that the latter is energetically more expensive, depending on the synthesis of new membranes, with the lack of L-lactate caused by glycogenolysis blockade impairing such stabilization, resulting in the overall presence of fewer, smaller spines, as measured by Golgi staining and 3D-EM.

As the spine density increase was blocked, the PSD surface area followed the same fate. PSD growth supposedly follows a signaling from the presynaptic recycling pool, which is recruited upon LTP (Bell et al. 2014). Analysis of presynaptic structures did not reveal major differences between control and DAB-treated mice in terms of boutons size and docked vesicle number (Fig. S6A,C,D,E; Fig. S7B and Table S7,S8). However, our findings showed that significant presynaptic structural plasticity occurs following inhibition of glycogenolysis. Indeed, the total number of vesicles decreased 24 hours after DAB application, suggesting that interfering with metabolic fluxes affected the cytosolic recycling vesicle pool, while the ready-releasable pool was unaffected (Fig. S6B; Fig. S7A and Table S7,S8). The reduced vesicular recycling pool might then be responsible for the impaired growth of the PSD surface. Although ultrastructural studies suggest that synaptic strength might be related to presynaptic size (Yeow and Peterson 1991; Pierce and Lewin 1994), more recent evidence showed that hippocampal LTP does not affect bouton size (Medvedev et al. 2010), in agreement with our observations. Interestingly, coadministration of L-lactate with DAB failed to rescue the recycling pool of vesicles; this observation is in agreement with the absence of increase in the PSD surface area in the L-lactate rescue experiments, suggesting a functional crosslink between the two.

It is noteworthy observing that learning induced a massive increase in the size of glycogen granules, partially impaired by DAB, in astrocytic profiles in proximity of synapses modified by learning. Previous work has shown how learning and LTP induce astrocytic processes plasticity in vivo and in vitro, in particular around potentiated synapses. For instance, using a whisker stimulation protocol (Genoud et al. 2006), astrocytic synaptic coverage increases significantly. Although literature from the last decade largely speculated that astrocytic plasticity, stimulated by extra synaptic glutamate, serves to confining glutamate spill over from larger, potentiated synapses (Witcher et al. 2007), we hypothesize that learning-dependent astrocytic plasticity might be driven by a higher demand of energy supply from potentiated synapses. Indeed, we have recently shown that glycogen granules are preferentially located in proximity of synapses (Calì et al. 2016; Coggan et al. 2018). The absence of increase in the size of granules as a consequence of the DAB treatment deserves an explanation, as at a first glance it might not be expected. DAB is indeed an inhibitor of GP (Latsis et al. 2002; Walls et al. 2008; Díaz-Lobo et al. 2016). Therefore, one would rather expect to observe accumulation of glycogen granules or even large clusters following inhibition of glycogenolysis, since DAB prevents the degradation of both the newly formed glycogen pool and the one already present in the astrocytes, as observed 24 hours following learning. However, DAB has also been shown to inhibit glycogen synthase, thus effectively "freezing" glycogen turnover. Moreover, basal levels are already low. Another possible explanation might be that DAB resulted in the lack of LTP and LTM, which possibly are the signals for glycogen cluster resynthesis. LTM in dorsal hippocampus, in particular, has been shown to depend on noradrenergic signaling; the blockade of astrocytic β2 adrenergic receptors, whose activation has a potent glycogenolytic effect (Sorg and Magistretti 1991), had an amnestic effect similar to DAB (Gao et al. 2016). Failed LTM, which is associated with the failure to maintain LTP (Suzuki et al. 2011), has also an impact on astrocytic structural rearrangement. Thus both in the presence of DAB, the number of glycogen granules and their volume density dropped, the latter by about 56%.

In order to evaluate the impact of lactate on the behavioral and structural phenotypes affected by DAB, we attempted to rescue them by an acute phasic injection of L-lactate, together with DAB. The behavioral phenotype was rescued, since L-lactate injection bypasses the impaired glycogen-dependent ANLS. Given the recovery of the behavioral phenotype, it is not surprising that we also observed a rescue of the density of spines, an observation which is consistent with the rescue of the turnover of new spines in the in vitro model of LTP.

However, we did not observe a recovery in the size of the spines and of the PSD, nor of the presynaptic recycling pool. These observations might be related to the lack of L-lactate in rescuing glycogen granules size and density in the same conditions, which is not surprising, as lactate is not a substrate for glycogen.

Our results suggest a sequence of events, whereby long-term memory and LTP at 24 hours mainly rely on an increase in the number of spines requiring an adequate energy supply most likely needed for protein synthesis. In vivo electrophysiological recordings have shown that LTP induction is not sensitive to DAB but that DAB blocks LTP maintenance in a manner that can be rescued by lactate (Suzuki et al. 2011). Results reported here on a behavioral NOR test are consistent with previous reports showing the dependence of learning on lactate derived from glycogen (Gibbs et al. 2006; Newman et al. 2011; Suzuki et al. 2011; Boury-Jamot et al. 2016).

Altogether, these results indicate that glycogen-derived L-lactate plays a major role in memory consolidation and suggest that its presence acts through powering structural stabilization of newly formed spines in hippocampal neurons. Our observations on the structural rearrangement of the neuropil also indicate that an energy-deficient network might not be structurally ready to stabilize long-term memory. On the astrocytic side, these results show that the size and density increase of

Downloaded from https://academic.oup.com/cercor/article-abstract/30/4/2114/5625994 by guest on 24 June 2020

glycogen granules in astrocytes can be taken as a marker for the potentiated synapses that they ensheath.

Supplementary Material

Supplementary material can be found at *Cerebral Cortex* online.

Funding

"KAUST-EPFL Alliance for Brain Energy Metabolism"(CRG KAUST Grant to P.J.M.); KAUST Baseline (to A.F. and P.J.M.).

Notes

We thank Hubert Fiumelli (BESE, KAUST) and Marco Agus (VCC, KAUST) for constructive criticism of the manuscript and Daniya Boges and Kalpana Kare (BESE, KAUST) for the technical support for the reconstructions and analysis. We also thank Prof. Eugenio Scanziani (University of Milan, Milano, Italy) for the technical support for imaging of Evans blue and hematoxylin and eosin-stained sections. *Conflict of Interest*: The authors declare no competing interests.

Author Contributions

All 3D electron microscopy investigations were performed by A.F., E.S., and E.V. E.V. prepared all tissues in view of both the Golgi staining and the electron microscopy investigation, performed the 2D electron microscopy imaging, the Golgi staining, and all the related data formal analysis. Mice injections were performed by L.P., D.B., and M.S. Behavioral investigations were conceptualized, and their related formal analysis was performed by L.P., M.S., and D.B. Organotypic slice investigations were conceptualized by P.J.M., D.M., and M.D.R., supervised by D.M., and all related experiments and formal analysis were done by M.D.R. C.C. conceptualized the work on 3D reconstructions of glycogen granules and supervised N.G., who curated and analyzed the data. M.F. was involved as PhD Italian cosupervisor of E.V., while A.F. supervised the work of E.V. in all phases performed in KAUST. C.C. wrote the original draft of the paper, that was further edited and finalized together with E.V., A.F., and P.J.M. A.F. and P.J.M. conceived the work's main aim, which was then further conceptualized together with E.V. and C.C. All authors read and approved the manuscript.

Data and materials availability

All data are available in the main text and the Supplementary figures and tables.

References

Allaman I, Pellerin L, Magistretti PJ. 2000. Protein targeting to glycogen mRNA expression is stimulated by noradrenaline in mouse cortical astrocytes. *Glia*. 30(4):382–391.

Allaman I, Fiumelli H, Magistretti PJ, Martin JL. 2011. Fluoxetine regulates the expression of neurotrophic/growth factors and glucose metabolism in astrocytes. *Psychopharmacology (Berl.)*. 216(1):75–84.

Bell ME, *et al*. 2014. Dynamics of nascent and active zone ultrastructure as synapses enlarge during long-term potentiation in mature hippocampus. *J. Comp. Neurol*. 522(17):3861–3884.

Bourne J, Harris KM. 2007. Do thin spines learn to be mushroom spines that remember? *Curr. Opin. Neurobiol*. 17(3):381–386.

Bourne JN, Harris KM. 2011. Coordination of size and number of excitatory and inhibitory synapses results in a balanced structural plasticity along mature hippocampal CA1 dendrites during LTP. *Hippocampus*. 21(4):354–373.

Boury-Jamot B, *et al*. 2016. Disrupting astrocyte-neuron lactate transfer persistently reduces conditioned responses to cocaine. *Mol. Psychiatry*. 21(8):1070–1076.

Calì C, *et al*. 2016. Three-dimensional immersive virtual reality for studying cellular compartments in 3D models from EM preparations of neural tissues. *J. Comp. Neurol*. 524(1): 23–38.

Calì C, *et al*. 2018. The effects of aging on neuropil structure in mouse somatosensory cortex—a 3D electron microscopy analysis of layer 1. *PloS One*. 13(7):e0198131.

Calì C, Tauffenberger A, Magistretti PJ. 2019. The strategic location of glycogen and lactate: from body energy reserve to brain plasticity. *Front. Cell. Neurosci*. 13:82.

Cardinaux JR, Magistretti PJ. 1996. Vasoactive intestinal peptide, pituitary adenylate cyclase activating peptide, and noradrenaline induce the transcription factors CCAAT/enhancer binding protein (C/EBP)-beta and C/EBP delta in mouse cortical astrocytes: involvement in cAMP-regulated glycogen metabolism. *J. Neurosci*. 16(3):919–929.

Chuquet J, Quilichini P, Nimchinsky EA, Buzsáki G. 2010. Predominant enhancement of glucose uptake in astrocytes versus neurons during activation of the somatosensory cortex. *J. Neurosci*. 30(45):15298–15303.

Coggan JS, *et al*. 2018. Norepinephrine stimulates glycogenolysis in astrocytes to fuel neurons with lactate. *PLoS Comput. Biol*. 14(8):e1006392.

De Roo M, Klauser P, Muller D. 2008a. LTP promotes a selective long-term stabilization and clustering of dendritic spines. *PLoS Biol*. 6(9):e219.

De Roo M, Klauser P, Mendez P, Poglia L, Muller D. 2008b. Activity-dependent PSD formation and stabilization of newly formed spines in hippocampal slice cultures. *Cereb. Cortex*. 18(1):15161.

De Roo M, *et al*. 2009. Anesthetics rapidly promote synaptogenesis during a critical period of brain development. *PloS One*. 4(9):e7043.

De Roo M, Ribic A. 2017. Analyzing structural plasticity of dendritic spines in Organotypic slice culture. *Methods Mol. Biol*. 1538:277–289.

Díaz-Lobo M, *et al*. 2016. Inhibitory properties of 1, 4-dideoxy-1, 4-imino-D-arabinitol (DAB) derivatives acting on glycogen metabolising enzymes. *Org. Biomol. Chem*. 14(38): 9105–9113.

Drachman DA. 2005. Do we have brain to spare? *Neurology*. 64:2004–2005.

Dringen R, Hamprecht B. 1992. Glucose, insulin, and insulin-like growth factor I regulate the glycogen content of astroglia-rich primary cultures. *J. Neurochem*. 58(2):511–517.

Duarte JM, Lei H, Mlynárik V, Gruetter R. 2012. The neurochemical profile quantified by in vivo1H NMR spectroscopy. *Neuroimage*. 61(2):342–362.

Fox PT, Raichle ME, Mintun MA, Dence C. 1988. Nonoxidative glucose consumption during focal physiologic neural activity. *Science*. 241(4864):462–464.

Gao V, *et al*. 2016. Astrocytic β2-adrenergic receptors mediate hippocampal long-term memory consolidation. *Proc. Natl. Acad. Sci. USA*. 113(30):8526–8531.

Downloaded from https://academic.oup.com/cercor/article-abstract/30/4/2114/5625994 by guest on 24 June 2020

Genoud C, Quairiaux C, Steiner P, Hirling H, Welker E, Knott GW. 2006. Plasticity of astrocytic coverage and glutamate transporter expression in adult mouse cortex. *PLoS Biol*. 4(11):e343.

Gibbs ME, Anderson DG, Hertz L. 2006. Inhibition of glycogenolysis in astrocytes interrupts memory consolidation in young chickens. *Glia*. 54(3):214–222.

Hammond RS, Tull LE, Stackman RW. 2004. On the delay-dependent involvement of the hippocampus in object recognition memory. *Neurobiol. Learn. Mem*. 82(1):26–34.

Harris JJ, Jolivet R, Attwell D. 2012. Synaptic energy use and supply. *Neuron*. 75(5):762–777.

Hui S, *et al*. 2017. Glucose feeds the TCA cycle via circulating lactate. *Nature*. 551(7678):115–118.

Korol DL, Gardner RS, Tunur T, Gold PE. 2019. Involvement of lactate transport in two object recognition tasks that require either the hippocampus or striatum. *Behav. Neurosci*. 133(2):176.

Krieglstein J, Stock R. 1973. Comparative study of the effects of chloral hydrate and trichloroethanol on cerebral metabolism. *Naunyn Schmiedebergs Arch Pharmacol*. 277(4):323–332.

Lamprecht R, LeDoux J. 2004. Structural plasticity and memory. *Nat. Rev. Neurosci*. 5(1):45–54.

Latsis T, Andersen B, Agius L. 2002. Diverse effects of two allosteric inhibitors on the phosphorylation state of glycogen phosphorylase in hepatocytes. *Biochem J*. 368(1): 309–316.

Leuner B, Shors TJ. 2004. New spines, new memories. *Mol. Neurobiol*. 29(2):117–130.

Magistretti PJ, Morrison JH, Shoemaker WJ, Sapin V, Bloom FE. 1981. Vasoactive intestinal polypeptide induces glycogenolysis in mouse cortical slices: a possible regulatory mechanism for the local control of energy metabolism. *Proc. Natl. Acad. Sci. USA*. 78(10):6535–6539.

Magistretti PJ, Morrison JH. 1988. Noradrenaline- and vasoactive intestinal peptide-containing neuronal systems in neocortex: functional convergence with contrasting morphology. *Neuroscience*. 24(2):367–378.

Magistretti PJ, Allaman I. 2013. Brain energy metabolism. In: *Neuroscience in the 21st century: from basic to clinical*, pp. 1591–1620.

Magistretti PJ, Allaman I. 2015. A cellular perspective on brain energy metabolism and functional imaging. *Neuron*. 86(4):883–901.

Magistretti PJ, Allaman I. 2018. Lactate in the brain: from metabolic end-product to signalling molecule. *Nat. Rev. Neurosci*. 19(4):235–249.

Marchand I, Chorneyko K, Tarnopolsky M, Hamilton S, Shearer J, Potvin J, Graham TE. 2002. Quantification of subcellular glycogen in resting human muscle: granule size, number, and location. *J. Appl. Physiol*. 93(5):1598–1607.

Margineanu MB, Mahmood H, Fiumelli H, Magistretti PJ. 2018. L-lactate regulates the expression of synaptic plasticity and neuroprotection genes in cortical neurons: a transcriptome analysis. *Front. Mol. Neurosci*. 11:375.

Medvedev NI, *et al*. 2010. Alterations in synaptic curvature in the dentate gyrus following induction of long-term potentiation, long-term depression, and treatment with the N-methyl-D-aspartate receptor antagonist CPP. *Neuroscience*. 171(2):390–397.

Medvedev NI, *et al*. 2014. Multiple spine boutons are formed after long-lasting LTP in the awake rat. *Brain Struct. Funct*. 219(1):407–414.

Menna E, *et al*. 2013. Eps8 controls dendritic spine density and synaptic plasticity through its actin-capping activity. *EMBO J*. 32(12):1730–1744.

Muller D, Toni N, Buchs PA. 2000. Spine changes associated with long-term potentiation. *Hippocampus*. 10(5):596–604.

Mumby DG. 2001. Perspectives on object-recognition memory following hippocampal damage: lessons from studies in rats. *Behav. Brain Res*. 127(1–2):159–181.

Nelson SR, Schulz DW, Passonneau JV, Lowry OH. 1968. Control of glycogen levels in brain. *J. Neurochem*. 15(11):1271–1279.

Newman LA, Korol DL, Gold PE. 2011. Lactate produced by glycogenolysis in astrocytes regulates memory processing. *PLoS ONE*. 6(12):e28427.

Newman LA, Scavuzzo CJ, Gold PE, Korol DL. 2017. Training-induced elevations in extracellular lactate in hippocampus and striatum: dissociations by cognitive strategy and type of reward. *Neurobiol Learn Mem*. 137:142–153.

Oberheim NA, Goldman SA, Nedergaard M. 2012. Heterogeneity of astrocytic form and function. *Methods Mol. Biol*. 814: 23–45.

Oe Y, Tominaga-Yoshino K, Hasegawa S, Ogura A. 2013. Dendritic spine dynamics in synaptogenesis after repeated LTP inductions: dependence on pre-existing spine density. *Sci. Rep*. 3:1957.

Paxinos G, Franklin KBJ. 2001. *The mouse brain in stereotaxic coordinates*. San Diego: Academic Press.

Pellerin L, Magistretti PJ. 1994. Glutamate uptake into astrocytes stimulates aerobic glycolysis: a mechanism coupling neuronal activity to glucose utilization. *Proc. Natl. Acad. Sci. USA*. 91(22):10625–10629.

Phelps CH. 1972. Barbiturate-induced glycogen accumulation in brain. An electron microscopic study. *Brain Res*. 39(1):225–234.

Phelps CH. 1975. An ultrastructural study of methionine sulphoximine-induced glycogen accumulation in astrocytes of the mouse cerebral cortex. *J. Neurocytol*. 4(4):479–490.

Pierce JP, Lewin GR. 1994. An ultrastructural size principle. *Neuroscience*. 58(3):441–446.

Raichle ME, Gusnard DA. 2002. Appraising the brain's energy budget. *Proc. Natl. Acad. Sci. USA*. 99(16):10237–10239.

Raichle ME, Mintun MA. 2006. Brain work and brain imaging. *Annu. Rev. Neurosci*. 29:449–476.

Sakai C, *et al*. 2014. Species differences in the pharmacokinetic parameters of cytochrome P450 probe substrates between experimental animals, such as mice, rats, dogs, monkeys, and microminipigs, and humans. *J Drug Metab Toxicol*. 5(6).

Shulman RG, Rothman DL. 2001. 13C NMR of intermediary metabolism: implications for systemic physiology. *Annu. Rev. Physiol*. 63(1):15–48.

Sommer C, Straehle C, Koethe U, Hamprecht FA. 2011. Ilastik: Interactive learning and segmentation toolkit. In 2011 IEEE international symposium on biomedical imaging: From nano to macro 230233.

Sorg O, Magistretti PJ. 1991. Characterization of the glycogenolysis elicited by vasoactive intestinal peptide, noradrenaline and adenosine in primary cultures of mouse cerebral cortical astrocytes. *Brain Res*. 563(1–2):227–233.

Sorra KE, Harris KM. 1998. Stability in synapse number and size at 2 hr after long-term potentiation in hippocampal area CA1. *J. Neurosci*. 18(2):658–671.

Suzuki A, *et al*. 2011. Astrocyte-neuron lactate transport is required for long-term memory formation. *Cell*. 144(5):810–823.

Downloaded from https://academic.oup.com/cercor/article-abstract/30/4/2114/5625994 by guest on 24 June 2020

Takado Y, *et al*. 2015a. Imaging liver and brain glycogen metabolism at the nanometer scale. *Nanomedicine*. 11(1):239–245.

Takado Y, *et al*. 2015b. Imaging the time-integrated cerebral metabolic activity with subcellular resolution through nanometer-scale detection of biosynthetic products deriving from 13C-glucose. *J. Chem. Neuroanat*. 69:7–12.

Ventura R, Harris KM. 1999. Three-dimensional relationships between hippocampal synapses and astrocytes. *J. Neurosci*. 19(16):6897–6906.

Vohra R, Aldana BI, Waagepetersen H, Bergersen LH, Kolko M. 2019. Dual properties of lactate in Müller cells: the effect of GPR81 activation. *Invest. Ophthalmol. Vis. Sci*. 60(4):999–1008.

Voutsinos-Porche B, *et al*. 2003. Glial glutamate transporters mediate a functional metabolic crosstalk between neurons and astrocytes in the mouse developing cortex. *Neuron*. 37(2):275–286.

Walls AB, *et al*. 2008. Characterization of 1,4-dideoxy-1,4-imino-d-arabinitol (DAB) as an inhibitor of brain glycogen shunt activity. *J. Neurochem*. 105(4): 1462–1470.

Witcher MR, Kirov SA, Harris KM. 2007. Plasticity of perisynaptic astroglia during synaptogenesis in the mature rat hippocampus. *Glia*. 55(1):13–23.

Yang J, *et al*. 2014. Lactate promotes plasticity gene expression by potentiating NMDA signaling in neurons. *Proc. Natl. Acad. Sci. USA*. 111(33):12228–12233.

Yeow MBL, Peterson EH. 1991. Active zone organization and vesicle content scale with Bouton size at a vertebrate central synapse. *J. Comp. Neurol*. 307(3):475–486.

Downloaded from https://academic.oup.com/cercor/article-abstract/30/4/2114/5625994 by guest on 24 June 2020